06.3

Plane wave diffraction on a layer of asymmetric hyperbolic metamaterial

© M.V. Davidovich

Saratov National Research State University, Saratov, Russia
E-mail: DavidovichMV@info.sgu.ru

Received March 21, 2022
Revised October 3, 2022
Accepted October 25, 2022

We consider the diffraction of a plane wave on a layer of symmetric hyperbolic metamaterial made of metal and SiO_2 layers. It is shown that the reflection coefficient depends not only on the angle of incidence, but also on the direction of incidence relative to the anisotropy axis. In an arbitrary fall, a plate of an asymmetric hyperbolic metamaterial creates scattered waves of both polarizations.

Keywords: hyperbolic metamaterial, diffraction, effective permittivity tensor, homogenization.

DOI: 10.21883/TPL.2023.01.55337.19196

Hyperbolic metamaterials (HMMs) are uniaxial photonic crystals with their diagonalized effective permittivity tensor featuring diagonal components that have $\varepsilon'_\perp \varepsilon'_\parallel < 0$ [1]. Here, prime and double prime marks denote real negative imaginary parts, respectively; i.e., $\varepsilon_\perp = \varepsilon'_\perp - i\varepsilon''_\perp$ and $\varepsilon_\parallel = \varepsilon'_\parallel - i\varepsilon''_\parallel$. In addition, HMMs are viable at low losses ($\varepsilon''_\perp \ll |\varepsilon'_\perp|$, $\varepsilon''_\parallel \ll |\varepsilon'_\parallel|$) and moderate frequencies, since both these factors (including spatial dispersion (SD) that emerges at high frequencies) set bounds to the hyperbolic dispersion law [1]. The interest in metasurfaces and plasmon polaritons (PPs) along them [1–7] has been on the rise lately, since structures with surface PPs have a fairly wide application range. In the present study, we examine an asymmetric HMM layer that provides the possibility to control diffraction through parameter variation effected by altering the cut of interfaces (changing the orientation of the anisotropy axis). The inset of Fig. 1 shows an HMM plate with boundaries the normal to which makes a certain angle with the anisotropy axis. The HMM considered here is composed of alternating conducting and dielectric layers. Thin metal films or graphene sheets may serve as conducting layers. Under optical laser pumping, semiconducting and graphene films allow one to control diffraction optically [8]. Homogenization and derivation of effective permittivity are feasible in the low-frequency range at wavelengths $d_0 \ll \lambda$, where d_0 is the period. The Fresnel equation for an extraordinary wave takes the following form in this case: $k_\parallel^2/\varepsilon_\perp + k_\perp^2/\varepsilon_\parallel = k_0^2$ [1]. This approximation yields [1,9]

$$\varepsilon_{xx} = \varepsilon_{yy} = \frac{\varepsilon_1 t_1 + \varepsilon_2 t_2}{d_0}, \quad \varepsilon_{zz} = d_0 \left(\frac{t_1}{\varepsilon_1} + \frac{t_2}{\varepsilon_2} \right)^{-1}. \quad (1)$$

Here, $d_0 = t_1 + t_2$ is the structure period. It is possible to take SD into account, but the resulting relations are more complex. This can be done using, e.g., the following formulae [1,10]:

$$\varepsilon_{xx} = \varepsilon_{yy} = k_0^{-2} \Big[k^2/2 + k_{1z}^2 t^{-2} \big(t_1^2 + t_1 t_2 \big) + k_{2z}^2 t^{-2} \big(t_2^2 + t_1 t_2 \big) \Big], \quad (2)$$

$$\varepsilon_{zz} = k_0^{-2} k^2 \times \left\{ 1 - \frac{k_{1z}^2 d_0^{-2} (t_1^2 + t_1 t_2 \varepsilon_2/\varepsilon_1) + k_{2z}^2 d_0^{-2} (t_2^2 + t_1 t_2 \varepsilon_1/\varepsilon_2)}{k^2/2 + k_{1z}^2 d_0^{-2} (t_1^2 + t_1 t_2) + k_{2z}^2 d_0^{-2} (t_2^2 + t_1 t_2)} \right\}^{-1}. \quad (3)$$

Here, $k_{1z}^2 = k_0^2 \varepsilon_1 - k^2$, $k_{2z}^2 = k_0^2 \varepsilon_2 - k^2$. At $t_1 = t_2 = d_0/2$, relations (2) and (3) match formulae (1) and yield $\varepsilon_{xx} = \varepsilon_{yy} = (\varepsilon_1 + \varepsilon_2)/2$, $\varepsilon_{zz} = 2\varepsilon_1\varepsilon_2/(\varepsilon_1 + \varepsilon_2)$. Let us use the Drude–Lorentz model for permittivity of metal films. In the optical range, the thicknesses of layers should be on the order of tens of nanometers. The hyperbolicity conditions are satisfied in this case within certain regions. An HMM may be produced [1] using alternating metal and dielectric layers with $t_1 = t_m$, $t_2 = t_d$ and permittivities $\varepsilon'_m(\omega) < 0$ and $\varepsilon'_d(\omega) > 1$ of metal and dielectric materials, respectively. Here and elsewhere, symbols m and d stand for „metal" and „dielectric." Setting $t_1 = t_2 = d/2$, we find $\varepsilon_{xx} = \varepsilon_{yy} = (\varepsilon'_m + \varepsilon'_d)/2$, $\varepsilon_{zz} = 2\varepsilon'_m\varepsilon'_d/(\varepsilon'_m + \varepsilon'_d)$. Both HMM types may be produced (depending on the sign of $\varepsilon'_m + \varepsilon'_d$) in the region where $\varepsilon'_m(\omega) < 0$. Rotating the HMM anisotropy axis by an angle of α, we alter permittivity tensor $\hat{\varepsilon}(\alpha) = \hat{T}^{-1}(\alpha)\hat{\varepsilon}(0)\hat{T}(\alpha)$ in the way specified by rotation matrix $\hat{T}(\alpha)$, thus inducing the emergence of nondiagonal terms. The propagation of plasmons in a film of this asymmetric HMM depends on the rotation angle and is complex in nature [11]. Here, we illustrate the behavior of reflection R and transmission T coefficients of a plane wave at different rotation angles and angles of incidence (Fig. 1) on an asymmetric HMM layer. The region of excitation of plasmons corresponds to the $|R|$ minimum. A specific angle of wave incidence ϕ, which establishes a match between the

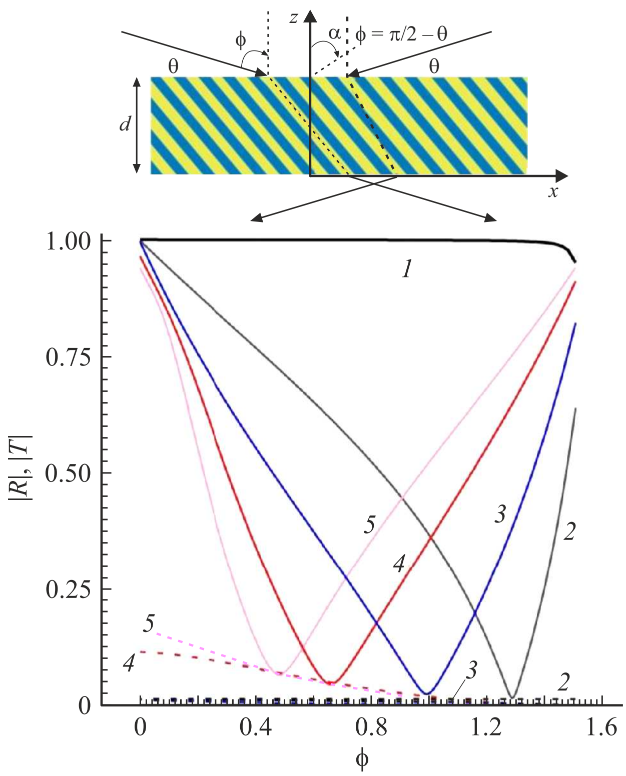

Figure 1. Dependences of moduli of reflection $|R|$ (solid curves) and transmission $|T|$ (dashed curves) coefficients on incidence angle ϕ for an HMM structure with $d = 420$ nm, $t_m = t_d = 20$ nm, $\varepsilon_d = 3$ at rotation angle $\alpha = 0$ (*1*), $\pi/12$ (*2*), $\pi/8$ (*3*), $\pi/4$ (*4*), $\pi/3$ (*5*).

PP phase velocity and the speed of wave energy transport in a layer, is needed for their efficient excitation. Asymmetry emerges with respect to incidence from different directions relative to the normal.

To derive Fresnel formulae, we consider the matrix of rotation about axis y by an angle of α:

$$\hat{T}_y(\alpha) = \begin{bmatrix} \cos\alpha & 0 & -\sin\alpha \\ 0 & 1 & 0 \\ \sin\alpha & 0 & \cos\alpha \end{bmatrix}. \quad (4)$$

Acting on vector $\mathbf{E}$, this matrix yields $E'_x = E_x \cos\alpha - E_z \sin\alpha$, $E'_y = E_y$, $E'_z = E_x \sin\alpha + E_z \cos\alpha$; i.e., this is a counterclockwise rotation. The initial permittivity matrix then takes the form

$$\tilde{\varepsilon} = \hat{T}_y^{-1}(\alpha)\hat{\varepsilon}\hat{T}_y(\alpha) = \hat{T}_y(-\alpha)\hat{\varepsilon}\hat{T}_y(\alpha)$$

or

$$\tilde{\varepsilon}_{xx} = \cos^2(\alpha)\varepsilon_{xx} + \sin^2(\alpha)\varepsilon_{zz},$$
$$\tilde{\varepsilon}_{zz} = \cos^2(\alpha)\varepsilon_{zz} + \sin^2(\alpha)\varepsilon_{xx},$$
$$\tilde{\varepsilon}_{xz} = \sin\alpha\cos\alpha(\varepsilon_{zz} - \varepsilon_{xx}).$$

Here $\varepsilon_{xx} = \varepsilon_{yy} = \varepsilon_\perp$, $\varepsilon_{zz} = \varepsilon_\parallel$.

Let us derive Fresnel formulae for a plane wave with p and s polarizations incident at angle ϕ from below onto a structure in the form of a layer with arbitrary angle α. The Maxwell equations in a medium with permittivity tensor $\tilde{\varepsilon}$ are written as $\hat{k}\mathbf{H} = \omega\varepsilon_0\hat{\varepsilon}\mathbf{E}$, $-\hat{k}\mathbf{E} = \omega\mu_0\hat{I}\mathbf{H}$, where matrix $\hat{k}$ was given in [1]. It corresponds to the „rotor“operator. This expression holds true for any tensor $\hat{\varepsilon}$ (nondiagonal tensors included). In the case of a rotated tensor, it takes the form

$$k_z H_y - k_y H_z = \omega\varepsilon_0(\tilde{\varepsilon}_{xx}E_x + \tilde{\varepsilon}_{xz}E_z),$$
$$E_x = \frac{k_z H_y - k_y H_z - \omega\varepsilon_0\tilde{\varepsilon}_{xz}E_z}{\omega\varepsilon_0\tilde{\varepsilon}_{xx}}, \quad (5a)$$

$$k_x H_z - k_z H_x = \omega\varepsilon_0\varepsilon_{xx}E_y, \; E_y = \frac{k_x H_z - k_z H_x}{\omega\varepsilon_0\varepsilon_{yy}}, \quad (5b)$$

$$k_y H_x - k_x H_y - \omega\varepsilon_0(\tilde{\varepsilon}_{xz}E_x + \tilde{\varepsilon}_{zz}E_z), \quad (5c)$$

$$k_y E_z - k_z E_y = \omega\mu_0 H_x, \qquad H_x = \frac{k_y E_z - k_z E_y}{\omega\mu_0}, \quad (5d)$$

$$k_z E_x - k_x E_z = \omega\mu_0 H_y, \qquad H_y = \frac{k_z E_x - k_x E_z}{\omega\mu_0}, \quad (5e)$$

$$k_x E_y - k_y E_x = \omega\mu_0 H_z. \quad (5f)$$

Equations (5a), (5b), (5d), (5e) are written in two equivalent forms, where the second formulae are for field components transverse to direction z. Inserting these magnetic components from (5e) into (5a) and from (5d) into (5b) and then transverse electric field components from (5a) into (5e) and from (5b) into (5d), we find transverse components E_x, E_y, H_x, H_y. Inserting them into (5c) and (5f), we obtain

$$-k_y\left(\frac{k_x k_z}{k_0^2\varepsilon_{yy} - k_z k_z} + \frac{k_0^2\tilde{\varepsilon}_{xz} + k_z k_x}{k_z k_z - k_0^2\tilde{\varepsilon}_{xx}}\right)E_z$$
$$= \omega\mu_0\left(1 + \frac{k_y k_y}{k_z k_z - k_0^2\tilde{\varepsilon}_{xx}} - \frac{k_x k_x}{k_0^2\varepsilon_{yy} - k_z k_z}\right)H_z,$$

$$-k_y\left[\frac{k_z k_x}{k_0^2\varepsilon_{yy} - k_z k_z} + \frac{k_x k_z}{k_z k_z - k_0^2\tilde{\varepsilon}_{xx}} + \frac{k_0^2\tilde{\varepsilon}_{xz}}{k_z k_z - k_0^2\tilde{\varepsilon}_{xx}}\right]H_z$$
$$= \omega\varepsilon_0\left[\tilde{\varepsilon}_{zz} - \frac{\varepsilon_{xx}k_y k_y}{k_0^2\varepsilon_{yy} - k_z k_z} + \frac{\tilde{\varepsilon}_{xx}k_x k_x + \tilde{\varepsilon}_{xz}k_x k_z}{k_z k_z - k_0^2\tilde{\varepsilon}_{xx}}\right.$$
$$\left. + \frac{\tilde{\varepsilon}_{xz}(k_0^2\tilde{\varepsilon}_{xz} + k_z k_x)}{k_z k_z - k_0^2\tilde{\varepsilon}_{xx}}\right]E_z.$$

The zero determinant of this system is the Fresnel equation. Let us set $\Delta_{\tilde{\varepsilon}} = \tilde{\varepsilon}_{xx}\tilde{\varepsilon}_{zz} - \tilde{\varepsilon}_{xz}^2$. This equation is of interest at $k_y = 0$, when it splits into two parts:

$$k_x^\pm = \pm\sqrt{k_0^2\varepsilon_{yy} - k_z^2}, \quad (6)$$

$$k_x^\pm = \frac{-k_z\tilde{\varepsilon}_{xz} \pm \sqrt{(k_0^2\tilde{\varepsilon}_{xx} - k_z^2)\Delta_{\tilde{\varepsilon}}}}{\tilde{\varepsilon}_{xx}}. \quad (7)$$

The first equation corresponds to an H wave with components H_z, H_x, and E_y. It may be excited by an s-polarized wave. An H wave of the opposite direction features component $k_z^- = -k_z^+ = -k_z$, and the same value of k_x corresponds to it. The $k_x^{\pm} = \pm k_x$ values specify the direction of wave incidence (to the left or to the right of the normal). The second equation corresponds to an E wave with components E_z, E_x, and H_y. It is excited by an incident p-polarized wave. It has different $k_x^{\pm}$, and a wave travelling in the opposite direction along axis x features component k_x^-. The values of k_x are real. A wave travelling in the opposite direction along axis z features component k_z^{+-} or k_z^{--} (depending on the direction of wave propagation along axis x). The first index denotes the k_x direction. The wave opposite in the z direction has $\mathrm{Re}(k_z^{\pm-}) < 0$. Let $k_x = k_x^+ > 0$ be the value in an incident wave and be specified by the following relation:

$$k_x = k_x^+ = \frac{-k_z^{\pm}\tilde{\varepsilon}_{xz} \pm \sqrt{(k_0^2\tilde{\varepsilon}_{xx} - k_z^{\pm 2})\Delta_{\tilde{\varepsilon}}}}{\tilde{\varepsilon}_{xx}} > 0.$$

We assume that $k_x = k_x^+ > 0$. If the direction of incidence relative to the normal is reversed,

$$-k_x = k_x^- = \frac{k_z^{\pm}\tilde{\varepsilon}_{xz} \mp \sqrt{(k_0^2\tilde{\varepsilon}_{xx} - k_z^{\pm 2})\Delta_{\tilde{\varepsilon}}}}{\tilde{\varepsilon}_{xx}} < 0.$$

The $k_x^{\pm}$ values specify the direction of wave incidence (to the left or to the right of the normal). Instead of (7), we may use equation

$$k_z^{\pm} = -(\tilde{\varepsilon}_{xz}/\tilde{\varepsilon}_{zz})k_x \pm \sqrt{(\tilde{\varepsilon}_{xx} - \tilde{\varepsilon}_{xz}^2/\tilde{\varepsilon}_{zz})k_0^2 - \left[(\tilde{\varepsilon}_{xx}/\tilde{\varepsilon}_{zz}) - (\tilde{\varepsilon}_{xz}/\tilde{\varepsilon}_{zz})^2\right]k_x^2}. \quad (8)$$

It assumes form $k_z^{\pm} = \pm\sqrt{k_0^2\tilde{\varepsilon}_{xx} - k_x^2\tilde{\varepsilon}_{xx}/\tilde{\varepsilon}_{zz}}$ for a diagonal tensor ($\alpha = 0$); i.e., $k_z^{\pm}$ define opposing (and independent of the sign of k_x) components of oppositely directed waves. In the general case (8), they depend on the sign of k_x. The sign in (8) should be chosen according to $\mathrm{Re}(k_z^+) > 0$. Let us use the impedance approach. The wave below is

$$E_q = \left[\exp(-ik_{0z}z) + R_q\exp(ik_{0z}z)\right]\exp(-ik_xx),$$

$$Z_0H_q = \left[\exp(-ik_{0z}z) - R_q\exp(ik_{0z}z)\right]\exp(-ik_xx)/\rho_{0q}.$$

The wave above is given by

$$E_q = T_q\exp\bigl(-ik_{0z}(z-d) - ik_xx\bigr),$$

$$Z_0H_q = T_q\exp(-ik_{0z}(z-d) - ik_xx)/\rho_{0q}.$$

In the structure (layer),

$$E_q = \left[A_q^+\exp\bigl(-ik_z^{++}z\bigr) + A_q^-\exp\bigl(-ik_z^{+-}z\bigr)\right]\exp\bigl(-ik_xx\bigr),$$

$$Z_0H_q = \left[A_q^+\exp\bigl(-ik_z^{++}z\bigr)/\rho_q^{++} - A_q^-\exp\bigl(-ik_z^{+-}z\bigr)/\rho_q^{+-}\right]\exp\bigl(-ik_xx\bigr).$$

The first plus should be changed for minus in the case of propagation along $-x$. At $q = p$, we obtain $E_q = E_x$, $H_q = H_y$, and

$$\rho_e^{++} = \frac{E_x}{Z_0H_y} = \frac{k_0^2\tilde{\varepsilon}_{xz} + k_z^{++}k_x^+}{k_0(\tilde{\varepsilon}_{xx}k_x^+ + \tilde{\varepsilon}_{xz}k_z^{++})},$$

$$\rho_e^{+-} = -\frac{E_x}{Z_0H_y} = -\frac{k_0^2\tilde{\varepsilon}_{xz} + k_z^{+-}k_x^+}{k_0(\tilde{\varepsilon}_{xx}k_x^+ + \tilde{\varepsilon}_{xz}k_z^{+-})}.$$

The first and the second signs correspond to axes x and z, respectively. If $\tilde{\varepsilon}_{xz} = 0$, $\rho_e^{++} = \rho_e^{+-} = k_z^{++}/(\omega\varepsilon_0\tilde{\varepsilon}_{xx})$ $k_z^{++} = -k_z^{+-}$. Sewing the fields together, we find $1 + R_e^+ = A_e^+ + A_e^-$, $1 - R_e^+ = A_e^+\rho_{0e}/\rho_e^{++} - A_e^-\rho_{0e}/\rho_e^{+-}$; in this case,

$$A_e^+\exp(-ik_z^{++}d) + A_e^-\exp(-ik_z^{+-}d) = T_e^+, \quad (9)$$

$$A_e^+\exp(-ik_z^{++}d)\rho_{0e}/\rho_e^{++} - A_e^-\exp(-ik_z^{+-}d)\rho_{0e}/\rho_e^{-+} = T_e^+. \quad (10)$$

Summing up the first two equations, we obtain

$$A_e^+(1 + \rho_{0e}/\rho_e^{++}) + A_e^-(1 - \rho_{0e}/\rho_e^{+-}) = 2.$$

The subtraction of the fourth equation from the third one yields

$$A_e^+\exp(-ik_z^{++}d)(1 - \rho_{0e}/\rho_e^{++}) + A_e^-\exp(-ik_z^{+-}d)(1 + \rho_{0e}/\rho_e^{+-}) = 0.$$

The solution of this system of equation takes the form

$$A_e^+ = 2(-ik_z^{+-}d)(1 + \rho_{0e}/\rho_e^{+-})/\Delta^+,$$

$$A_e^- = -2\exp(-ik_z^{++}d)(1 - \rho_{0e}/\rho_e^{++})/\Delta^+,$$

where the determinant is

$$\Delta^+ = (-ik_z^{+-}d)(1 + \rho_{0e}/\rho_e^{++})(1 + \rho_{0e}/\rho_e^{+-}) - \exp(-ik_z^{++}d)(1 - \rho_{0e}/\rho_e^{++})(1 - \rho_{0e}/\rho_e^{+-}).$$

The reflection coefficient is then written as

$$R_e^+ = 2\left\{\left[(-ik_z^{+-}d)(1 + \rho_{0e}/\rho_e^{-+}) - \exp(-ik_z^{++}d)(1 - \rho_{0e}/\rho_e^{++})\right]/\Delta^+\right\} - 1. \quad (11)$$

The reflection coefficient corresponding to propagation along $-x$ is

$$R_e^- = 2\left\{\left[(-ik_z^{--}d)(1 + \rho_{0e}/\rho_e^{--}) - \exp(-ik_z^{-+}d)(1 - \rho_{0e}/\rho_e^{-+})\right] / \Delta^-\right\} - 1, \quad (12)$$

$$\Delta^- = (-ik_z^{--}d)(1 + \rho_{0e}/\rho_e^{-+})(1 + \rho_{0e}/\rho_e^{--}) - \exp(-ik_z^{-+}d)(1 - \rho_{0e}/\rho_e^{-+})(1 - \rho_{0e}/\rho_e^{--}).$$

The following values should be chosen in these relations:

$$k_z^{\pm\pm} = -(\tilde{\varepsilon}_{xz}/\tilde{\varepsilon}_{zz})k_x^{\pm}$$

$$\pm\sqrt{(\tilde{\varepsilon}_{xx} - \tilde{\varepsilon}_{xz}^2/\tilde{\varepsilon}_{zz})k_0^2 - \left[(\tilde{\varepsilon}_{xx}/\tilde{\varepsilon}_{zz}) - (\tilde{\varepsilon}_{xz}/\tilde{\varepsilon}_{zz})^2\right]k_x^{\pm 2}},$$

$$\mathrm{Re}(k_z^{\pm+}) > 0, \qquad \mathrm{Re}(k_z^{\pm-}) < 0.$$

It can be seen that relations (9) and (10) remain unchanged under substitutions $k_z^{\pm+} \leftrightarrow k_z^{\pm-}$ and $A_e^+ \leftrightarrow A_e^-$ performed simultaneously; i.e., it does not matter which waves in a layer are assumed to be the direct and reverse ones. The values of $k_z^{\pm}$ derived from (8) at $k_x > 0$ and $k_x < 0$ differ. This suggests that different reflection coefficients correspond to equal incidence angles to the left and to the right of the normal. In physical terms, this follows from the fact that the electric vector under incidence from above and from the left (Fig. 1) is almost normal to thin metal sheets, thus yielding weak reflection. The structure acts as a set of plane-parallel waveguides. Since the electric vector under incidence at the same angle from above and from the right is almost tangent to metal layers, strong reflection is observed in this case. The transmission coefficient is

$$T_e^{\pm} = 2\left[\exp\left(-i(k_z^{\pm+} + k_z^{\pm-})d\right)(1 + \rho_{0e}/\rho_e^{\pm-})\right.$$

$$\left. - \exp\left(-i(k_z^{\pm-} + k_z^{\pm+})d\right)(1 - \rho_{0e}/\rho_e^{\pm+})\right] / \Delta^{\pm}.$$

According to (8), $k_z^{\pm+} + k_z^{\pm-} = -2(\tilde{\varepsilon}_{xz}/\tilde{\varepsilon}_{zz})k_x^{\pm}$; therefore,

$$T_e^{\pm} = 2\exp\left(2i(\tilde{\varepsilon}_{xz}/\tilde{\varepsilon}_{zz})k_x^{\pm}d\right)\rho_{0e}\frac{\rho_e^{\pm+} + \rho_e^{\pm-}}{\rho_e^{\pm+}\rho_e^{\pm-}\Delta^{\pm}}. \qquad (13)$$

At $\tilde{\varepsilon}_{xz} = 0$, we have $\rho_{e,h}^{\pm+} = \rho_{e,h}^{\pm-} = \rho_{e,h}$, $\rho_e = k_z/(k_0\tilde{\varepsilon}_{xx})$, $\rho_h = k_0/k_z$, and the known formula

$$T_{e,h}^{\pm} = \left[\cos(k_z d) + iW_{e,h}\sin(k_z d)\right]^{-1},$$

$$W_{e,h} = (\rho_{e,h}/\rho_{0e,h} + \rho_{0e,h}/\rho_{e,h})/2.$$

In an asymmetric HMM, both reflection and transmission of an E wave depend not only on the incidence angle value, but also on the positioning of the line of incidence relative to the normal. This is not true for the s polarization. In the general case of $k_y \neq 0$, waves are hybrid; i.e., reflected and transmitted waves of both polarizations are excited under incidence of a p- or s-polarized wave.

Thus, scattered waves of both polarizations emerge in diffraction by an HMM layer in the case of arbitrary anisotropy angle α and arbitrary wave incidence. In the considered scenario, this occurs at $k_y \neq 0$. In physical terms, this corresponds to the excitation of currents of all directions, which produce radiated waves of both polarizations, in metal layers. The calculations of $R = R_e$ and $T = T_e$ (Fig. 1) as functions of the incidence angle were performed for $\lambda = 500$ nm. Silver and SiO_2 layers were the materials tested. The permittivity of silver at the discussed wavelength is $\varepsilon_m = -8.23 - i0.287$. The value of $\varepsilon_d = 3$ was used as the permittivity of SiO_2. At equal layer thicknesses,

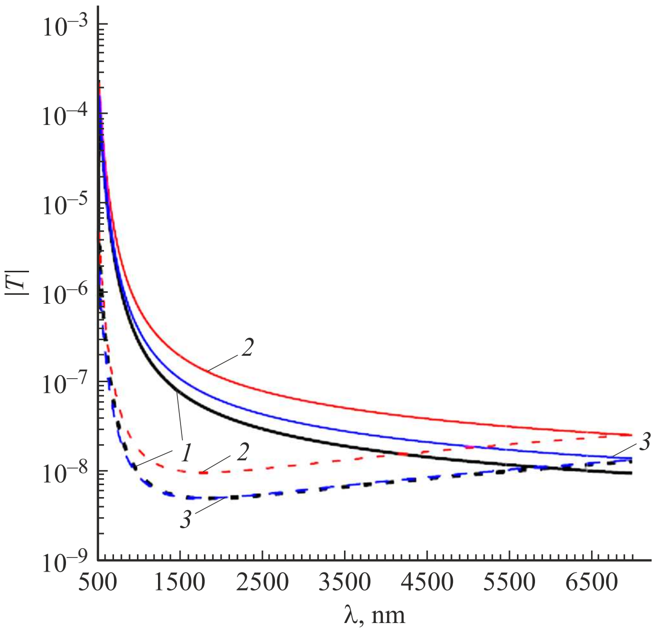

Figure 2. Moduli of transmission coefficients as functions of wavelength based on homogenization (dashed curves) and on a rigorous model (solid curves) for a structure with $t_m = t_d = 10$ nm, 22 periods, and a thickness of 440 nm. *1* — Normal incidence, *2* — incidence of an E mode, *3* — incidence of an H mode (the incidence angle is $\pi/4$).

$\varepsilon_{xx} = \varepsilon_{yy} = -2.62 - i0.144$ and $\varepsilon_{zz} = 9.431 - i0.1883$; i.e., the HMM condition is satisfied. Drude–Lorentz formula $\varepsilon_m(\omega) = \varepsilon_L - \omega_p^2/(\omega^2 - i\omega\omega_c)$ was used: $\varepsilon_L = 9.13$, $\omega_p = 1.57 \cdot 10^{16}$ Hz, and $\omega_c = 3.46 \cdot 10^{13}$ Hz. Its parameters were determined with regard to the density of conduction electrons and $\sigma_0 = \varepsilon_0\omega_p^2/\omega_c = 6.3 \cdot 10^7$ S/m for silver. This material features two zero-crossing points for $\varepsilon_m'(\omega)$. In our approximation, zero crossing occurs at a wavelength roughly equal to $\lambda = 345$ nm, which corresponds the first crossing. Figure 2 presents the comparison between an approximate solution based on homogenization and an exact solution at $\alpha = 0$ (i.e., when the anisotropy axis is aligned with axis z). The plasma frequencies of metals lie in the UV range, while the frequencies for semimetals and strongly doped semiconductors of the n-InSb kind may be reduced down to the THz range. Graphene–SiO_2 structures exhibit HMM properties in the same region [12]. Homogenization is 2–3 orders of magnitude more accurate in this setting. The considered asymmetric HMM layers may serve as polarization detectors or optical and IR screens. In the case of graphene, they may be controlled optically. The considered structure exhibits the maximum screening at a wavelength on the order of 900 nm.

Such problems are reduced to integral equations in the diffraction theory [13]. The finite impedance of ribbons may also be taken into account. However, a dielectric layer is hard to factor in: this requires the introduction of volume-surface integral equations. Plasmons along the considered

HMM layer were studied in [14]. The dispersion relation for plasmons reduces to the $R = 0$ condition. This is the Brewster condition under which a wave enters the structure without reflection, energy flows from vacuum into the layer from both sides, and k_x and k_{0z} become complex. A similar effect is observed in a nanowire HMM [14].

Funding

This study was supported by the Ministry of Education and Science of the Russian Federation under the state assignment (project No. FSRR-2020-0004).

Conflict of interest

The author declares that he has no conflict of interest.

References

[1] M.V. Davidovich, Phys. Usp., **62** (12), 1173 (2019). DOI: 10.3367/UFNe.2019.08.038643.
[2] N. Yu, F. Capasso, Nat. Mater, **13** (2), 139 (2014). DOI: 10.1038/NMAT3839
[3] Z. Li, K. Yao, F. Xia, S. Shen, J. Tian, Y. Liu, Sci. Rep., **5** (1), 12423 (2015). DOI: 10.1038/srep12423
[4] F. Lu, B. Liu, S. Shen, Adv. Opt. Mater., **2** (8), 794 (2014). DOI: 10.1002/adom.201400100
[5] K. Yao, Y. Liu, Nanotechnol. Rev., **3** (2), 177 (2014). DOI: 10.1515/ntrev-2012-0071
[6] Y. Liu, X. Zhang, Appl. Phys. Lett., **103** (14), 141101 (2013). DOI: 10.1063/1.4821444
[7] M.A. Remnev, V.V. Klimov, Phys. Usp., **61** (2), 157 (2018). DOI: 10.3367/UFNe.2017.08.038192.
[8] V. Ryzhii, M. Ryzhii, T. Otsuji, J. Appl. Phys., **101** (8), 083114 (2007). DOI: 10.1063/1.2717566
[9] S.M. Rytov, Sov. Phys. JETP, **2** (3), 446 (1956).
[10] M.V. Davidovich, JETP, **123** (6), 928 (2016). DOI: 10.7868/S0044451016120026.
[11] M.V. Davidovich, Komp'yut. Opt., **45** (1), 48 (2021) (in Russian). DOI: 10.18287/2412-6179-CO-673
[12] I.S. Nefedov, C.A. Valaginnopoulos, L.A. Melnikov, J. Opt., **15** (11), 114003 (2013). DOI: 10.1088/2040-8978/15/11/114003
[13] E.M. Nefedov, A.N. Sivov, *Elektrodinamika periodicheskikh struktur* (Nauka, M., 1977) (in Russian).
[14] D.G. Baranov, A.P. Vinogradov, K.R. Simovskii, I.S. Nefedov, S.A. Tret'yakov, JETP, **114** (4), 568 (2012). DOI: 10.1134/S106377611202001X.